RESEARCH ARTICLE

OPTICS

Why optics needs thickness

David A. B. Miller*

This study shows why and when optical systems need thickness as well as width or area. Wave diffraction explains the fundamental need for area or diameter of a lens or aperture to achieve some resolution or number of pixels in microscopes and cameras. This work demonstrates that if we know what the optics is to do, even before design, we can also deduce the minimum required thickness. This limit comes from diffraction combined with a concept called overlapping nonlocality *C* that can be deduced rigorously from just the mathematical description of what the device is to do. *C* expresses how much the input regions for different output regions overlap. This limit applies broadly to optics, from cameras to metasurfaces, and to wave systems generally.

Modern micro- and nanofabrication methods allow for the creation of complex optics well beyond historic lenses, mirrors, and prisms, giving optics that does what we want, not just what previous optics offered. Such complex designs can, however, require long calculations and may be difficult to fabricate. The complexity also makes it hard to anticipate what may be possible. So, we want simple limits to guide us. What minimum sizes might we need, for example? From diffraction, we understand how the minimum width or area of the optics must grow in proportion with the resolvable spots or pixels. However, there has been no corresponding basic understanding of how thick the optics must be or even why optics fundamentally might require thickness.

In this work, I show why optics and other wave systems may need thickness and derive quantitative limits. Optics may need to be nonlocal—the output at some point may need to depend on the inputs at many positions. Such nonlocality means that we need to communicate sideways within the structure or system. If we only need one such communication channel, one thin layer may be enough. However, if the input position ranges for one output point need to overlap with those for another output point, we have overlapping nonlocality (ONL). A key realization is that this ONL leads to thickness in optics.

Here, I introduce ONL and define it as the required number *C* of such sideways communication channels. A basic result is that the ONL comes from just the mathematical specification of what the device is to do. We can calculate *C* quite rigorously before starting design. Then, with some heuristics from diffraction, we can deduce minimum thicknesses or cross-sectional areas for the optics from *C*. This approach gives limits for many optical components, including imagers and metasurface structures for many possible applications. More generally, it bounds sizes for complex wave systems of any kind, including radio-frequency and acoustic systems.

Two recent questions in metasurfaces motivated this work. First, can we shrink the distance between a lens and the output plane in an imager—i.e., "squeezing space" (*1*), possibly with a spaceplate (*2*–*5*)? Second, what kinds of mathematical operations could we perform—for example, on an image—using some metasurface structure with some thickness (*6*–*8*)? This approach gives meaningful answers to these questions and others. It gives limits even for operation at just one frequency—so it is complementary to a spaceplate bandwidth limit (*4*) from the amount of material in the device (*9*, *10*)—and to related semiempirical limits (*11*). It also complements other recent limits on maximal enhancement of material response (*12*) and minimum thicknesses for local functions, such as perfect absorption (*12*) or reflection (*13*). Limits in optics and electromagnetics are of increasing interest (*14*). The concepts and results in our approach may allow different directions in this field and may find applications in other areas with complex optics, such as mode converters (*15*–*17*) and optical networks (*18*) in neural (*19*–*21*) and other (*22*–*24*) processing and interconnects (*25*).

An optical system (Fig. 1A) routes the light from an input surface to an output surface. Adding a dividing surface that mathematically cuts through both the input and output surfaces defines a transverse aperture. A minimum area or thickness for this aperture can be deduced by counting the number *C* of independent channels that must pass through it. For a camera or imager, we can evaluate *C* intuitively. Singular value decomposition (SVD) gives a rigorous mathematical approach for optical and wave systems generally.

ONL for imaging systems

An imager might have a lens surface as its input and an array of pixel sensors as its output. We take it to be nominally lossless—other than for incidental losses, such as weak background absorption, minor surface roughness scattering, or reflection losses—as it routes essentially all the relevant input power to the outputs. We also presume reciprocal optics—if waves can flow in one direction, then their phase conjugates can flow in the reverse direction with the same transmission factor.

An imager takes a set of N overlapping orthogonal inputs and maps them, one by one, to its N separate output pixels (see supplementary text S1 for extended discussion and proofs). We presume, as is typical for an imager, that the input power for each output pixel is distributed essentially uniformly over the input surface.

We now divide both input and output surfaces mathematically in half with surface S in the y-z plane. Now, an imager is very much larger than a wavelength. So, we presume we can construct new approximate basis sets for each half of the input surface, assigning a number of basis functions in proportion to the area of each part—so, $N/2$ input basis functions for each half. We presume that, in combination, this new divided pair of basis sets is approximately still able to describe all the N orthogonal input functions.

Now consider the mapping between the right half of the input surface and the left half of the output surface (Fig. 1D). Although $N/2$ orthogonal basis functions are associated with the right half of the input surface, we expect that half of those will be associated with forming images on the right half of the output plane. So, only $C_{RL} = N/4$ channels are associated with transferring power from the right half of the input plane to pixels on the left half of the output plane. Similarly, a number $C_{LR} = N/4$ of left-to-right channels are needed for waves from the left input surface to the right output surface.

In deducing the total number C of channels that must pass from right to left through the transverse aperture, we might think that we could neglect any left-to-right channels because they are going in the other direction. However, by reciprocity, associated with those $C_{LR} = N/4$ left-to-right channels, there must also be an equal number of reciprocal or backward versions of those channels from the output pixels on the right to the input surface on the left. So, altogether, we must physically allow for

$$C = C_{RL} + C_{LR} \quad (1)$$

channels crossing the dividing surface from right to left (or from left to right). In what follows, Eq. 1 applies quite generally. (Theoretically, nonreciprocal optics could eliminate the backward channels, reducing C by up to a factor

Ginzton Laboratory, Stanford University, Stanford, CA 94305, USA.
*Corresponding author. Email: dabm@stanford.edu

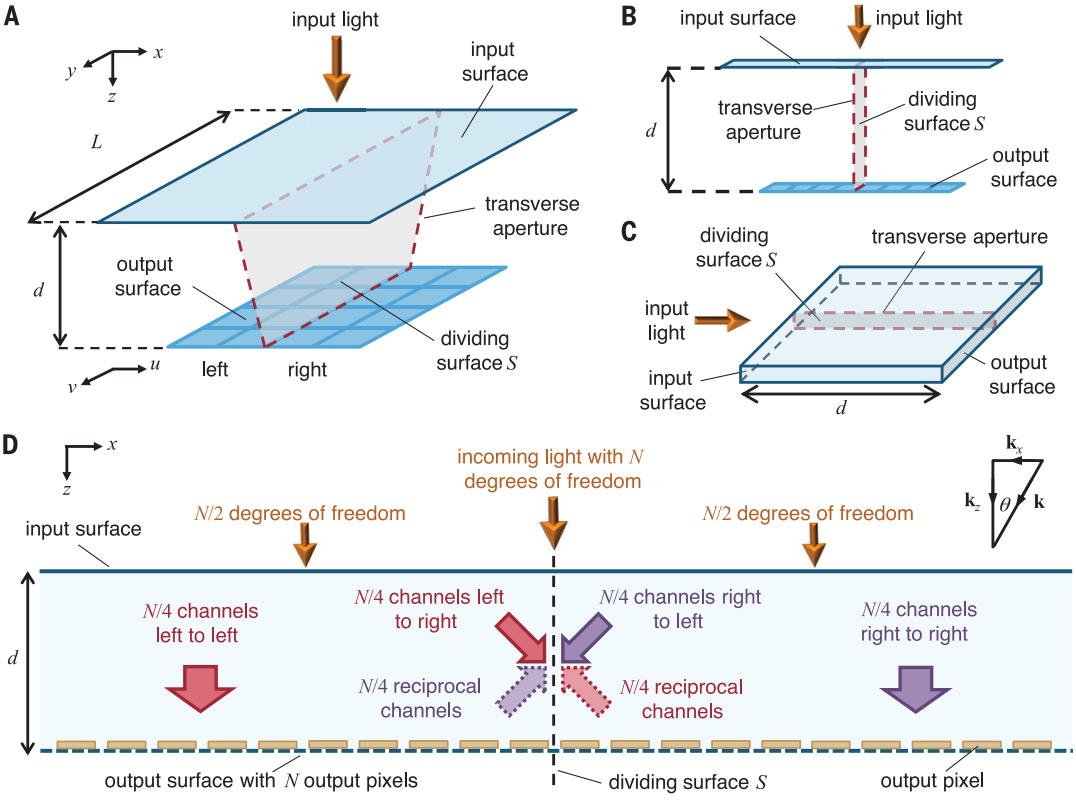

Fig. 1. Imaging systems and relevant surfaces and channels. (**A**) The input surface of an imaging system and the corresponding array of pixels on the output surface. We presume the surfaces are separated in z by some distance d. A dividing surface S that cuts through both input and output surfaces defines a transverse aperture. (**B** and **C**) A 1D imager, viewed either as a vertical slice that is thin in the y direction and has thickness d (B) or as a thin slab in the y direction with length d in x (C), as in a photonic integrated circuit. (**D**) Required internal channels when dividing an imaging system with a large number N of pixels and degrees of freedom into two equal parts.

of 2; see supplementary text S1). So, for our imager

$$C = N/4 + N/4 = N/2 \quad (2)$$

Note, C here comes from how an imager must work and the number of pixels, not from any specific design or size of the imager.

At this point, we can formally define ONL and C. The ONL C associated with a dividing surface S passing through the input and output surfaces is the number C of orthogonal channels that must cross from inputs on one side of S to outputs on the other side of S to implement the desired optical function, summing over both directions (left to right and right to left) of flow.

We emphasize that nonlocality itself does not require multiple channels. A single-mode optical fiber can have multiple taps spaced as far apart as we like. Appropriate light into those taps could be coherently combined to emerge at the fiber end, giving a very nonlocal system with only one channel. Rather, it is the overlapping nature of nonlocality in some systems—where different output points require different combinations of the light at some of the same input points—that necessitates multiple channels.

Required area or thickness of the transverse aperture

We presume that the optical systems of interest are sufficiently nonlocal that they require propagation of these C channels over transverse distances of many wavelengths in connecting input and output points (so we exclude any nearly local system, such as a very local differentiation just comparing inputs <1 wavelength apart). So, we presume propagating electromagnetic waves for these channels, not evanescent fields or near-field electromagnetic terms (*16*). We presume simple local dielectrics—the polarization at some point depends just on the field at that point—so we neglect any nonlocality from plasmons or other compound excitations. Thus, we can use wave diffraction heuristics to predict size limits. For simplicity, we effectively consider just one electromagnetic polarization, but the same results would apply to each polarization.

We start by pretending that the space between the input and output surfaces contains a uniform dielectric of refractive index n_r with light of free-space wavelength λ_o. Diffraction heuristics (supplementary text S2) tell us that in a narrow slit aperture, as in Fig. 1B, the maximum number of channels through the aperture corresponds to one for every $\lambda_o/2n_r$ of distance in the z direction. If this space is a nonuniform dielectric with maximum refractive index n_{max}, we conjecture at least $\lambda_o/2n_{max}$ per channel. Note, such a conjecture does not prove that no structure could do better. It is, however, consistent with typical behavior in the number of modes supported by slab waveguides, for example.

Practically, we may be limited to using only some fraction of the full 180° range of angles inside the structure—equivalently, a fraction α (≤1) of the available k-space (i.e., of the component k_z, as in Fig. 1D)—reducing the available channels proportionately. For example, if the internal angle is restricted to a range 0 to θ (Fig. 1D), then $\alpha = 1 - \cos\theta$. Hence, we conjecture in this one-dimensional (1D) case that we need a thickness

$$d \geq \frac{C\lambda_o}{2\alpha n_{max}} \quad (3)$$

We can extend this heuristic argument to the area A of a 2D transverse aperture, as in Fig. 1A, proposing

$$A \geq C\frac{1}{\alpha^2}\left(\frac{\lambda_o}{2n_{max}}\right)^2 \quad (4)$$

where we regard α^2 as the fraction of the 2D k_x,k_z k-space that we are practically able to use in design. Equation 4 is equivalent to an area of at least $(\lambda_o/2\alpha n_{max})^2$ for each channel through the transverse aperture.

Minimum thicknesses for imagers and related optical systems

We now apply Eqs. 3 and 4 to imagers. For a 1D imager with N_x pixels in a horizontal line in the x direction, as in Fig. 1, B and C, from Eq. 2, we have $C = N_x/2$, so from Eq. 3

$$d \geq \frac{N_x\lambda}{4\alpha n_{max}} \quad (5)$$

For a 2D imager, as in Fig. 1A, with N pixels (so $C = N/2$ from Eq. 2) and some characteristic width or diameter L, with transverse aperture area $A \sim Ld$, then from Eq. 4

$$d \geq \frac{N}{2L}\frac{1}{\alpha^2}\left(\frac{\lambda}{2n_{\max}}\right)^2 \quad (6)$$

To exploit the transverse aperture area in Eqs. 4 or 6 effectively, we may need to interleave degrees of freedom originally in x into the y dimension in the transverse aperture. This dimensional interleaving (DI) (supplementary text S3) is possible in optics, and we can design supercouplers to achieve it (supplementary text S4), including devising limits for these. Many approaches to optics, including free-space propagation, conventional imaging systems, simple dielectric stack structures, and 2D photonic crystals, do not, however, appear to support DI. In such cases, the thickness of these 2D systems may end up as the 1D limit (Eqs. 3 and 5).

We compare these limits on d with specific designs for imagers and spaceplates in supplementary text S5, showing that these limits are both obeyed and approached in existing optimized designs. A 12-megapixel smartphone camera (*26*) would require >~1.7-mm thickness if designed with typical (*26*) (<45°) maximum ray angles, even with no thickness in the lenses themselves (i.e., within about a factor of 3 of actual ~5-mm smartphone camera thicknesses). The multilayer spaceplate design in (*5*) has a designed thickness of 44.6 wavelengths, which is quite close to the predicted limit of 30 wavelengths.

An imager is a space-variant system—it looks different at different positions in the input or output. Several other such systems, such as Fourier transformers (*27*), mode sorters (*17*), and connection networks (*18*), can be analyzed similarly (supplementary text S6).

ONL for general linear optical devices

An imager or mode sorter has a pixelated output, which simplifies counting. Many optical devices, however, have no such pixelation, with continuous functions on input and output surfaces. The kernel—the linear operator relating the field at output points to that at input points—may be more local than the imager's global kernel; a spatial differentiator, which also may not be unitary, relates an output region to a small number of adjacent input regions (Fig. 2). The kernel may not be symmetric left to right, and it may not be obvious where to put the dividing surface. Fortunately, a SVD (*16*) approach is both compatible with the arguments so far and with these other cases.

With coordinates x and y on the input face and u and v on the output face (Fig. 1), as in the formalism of (*8*), generally

$$\Phi(u,v) = \iint D(u,v;x,y)\Psi(x,y)dxdy \quad (7)$$

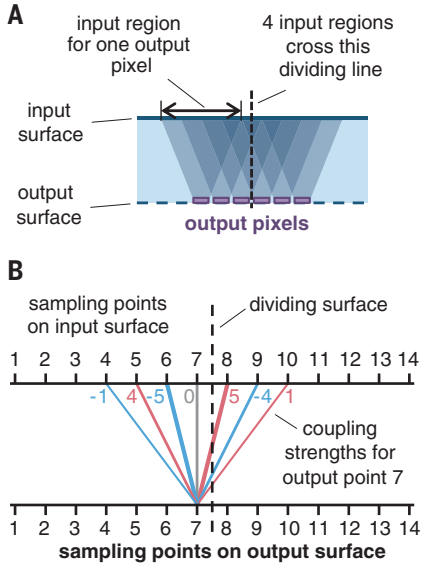

Fig. 2. Connections between input and output pixels. (**A**) A general example with an ONL of $C = 4$. (The trapezoids show which pixel is connected to which of the overlapping input regions.) (**B**) The coupling strengths between the input sampling points and the output sampling point 7 for a central finite-difference approximation to a fifth-order derivative. Coupling strengths for the other output points are shifted sideways as appropriate, as in (A).

where $D(u,v;x,y)$ is the kernel or the device operator (*15*, *16*), relating the output function $\Phi(u,v)$ to the input function $\Psi(x,y)$.

Choosing a dividing surface at input and output positions x_o and u_o, respectively, we have a divided operator D_{RL} restricted to the right part of the input and the corresponding left part of the output

$$D_{RL}(u,v;x,y) = \Theta(x-x_o)\Theta(u_o-u)D(u,v;x,y) \equiv \begin{cases} D(u,v;x,y) & u \leq u_o,\ x \geq x_o \\ 0 & u > u_o \\ 0 & x < x_o \end{cases} \quad (8)$$

where $\Theta(z)$ is the Heaviside (or step) function.

To find C, we start by finding the SVD of $D_{RL}(u,v;x,y)$. [Technically, we are establishing the necessary mode converter basis sets (*16*) to implement this right-to-left operator.] We then decide how many of the singular values (i.e., coupling strengths) have a magnitude above some small threshold and use that as the number of required right-to-left channels, C_{RL}. If necessary, from a corresponding left-to-right operator

$$D_{LR}(u,v;x,y) = \Theta(x_o-x)\Theta(u-u_o)D(u,v;x,y) \quad (9)$$

we similarly deduce a practical number of left-to-right channels C_{LR}. As above from Eq. 1, we add C_{RL} and C_{LR} to obtain C. For symmetric kernels, we may only need to calculate either C_{RL} or C_{LR} and double it.

If, for some kernel, it is not obvious where to put the dividing surface, we could repeat the calculation for all reasonable choices of dividing surface positions and choose the largest result for C. We should, however, keep the output central point u_o beneath its corresponding input range (supplementary text S7).

Constructing matrices for general linear optical devices

Because any such device operator D in a real physical system gives finite output for finite input, it is necessarily a Hilbert-Schmidt operator and hence is also compact (*16*, *28*). This means that it can be represented to any precision by a sufficiently large matrix $\mathbf{D}$.

The matrix elements of $\mathbf{D}$ are the couplings between specific chosen sampling points for the functions in the input and output spaces. Matrices $\mathbf{D}_{RL}$ and $\mathbf{D}_{LR}$ are then just truncated versions of $\mathbf{D}$; for example, for a 1D problem, $\mathbf{D}_{RL}$ and $\mathbf{D}_{LR}$ are just the upper-right and lower-left quadrants of $\mathbf{D}$. Standard matrix algebra gives the SVD of $\mathbf{D}_{RL}$ and, if necessary, that of $\mathbf{D}_{LR}$, which allows us to deduce C from Eq. 1. For pixelated optics, we could choose sampling points in the middle of each such pixel; essentially, we are then deducing limiting sizes for the optics so that it could give the right fields at least at these points.

For continuous functions and/or those without pixelation, we could just choose points with a separation that is close enough—intuitively sufficient to represent even the smallest bump in the function. The criterion for "close enough" is then that the number of singular values of the resulting matrices, above some chosen small threshold of relative magnitude, has converged. Increasing the density of sampling points beyond this makes essentially no difference to the resulting C. Generally, experience in the SVD description of optics (*16*) shows this behavior quite consistently, with convergence guaranteed by the operator compactness and associated sum rules (*16*, *28*).

In space-invariant optics (*8*), where the behavior depends only on the relative separation of input and output points, we are then convolving with a fixed kernel. Then, D simplifies (*8*) to

$$D(u,v;x,y) \rightarrow D(x-v,y-v) \quad (10)$$

Because the absolute position no longer matters, we simply choose one specific position for the calculations—e.g., for the output, such as $u = 0$, $v = 0$—and evaluate the matrices as required.

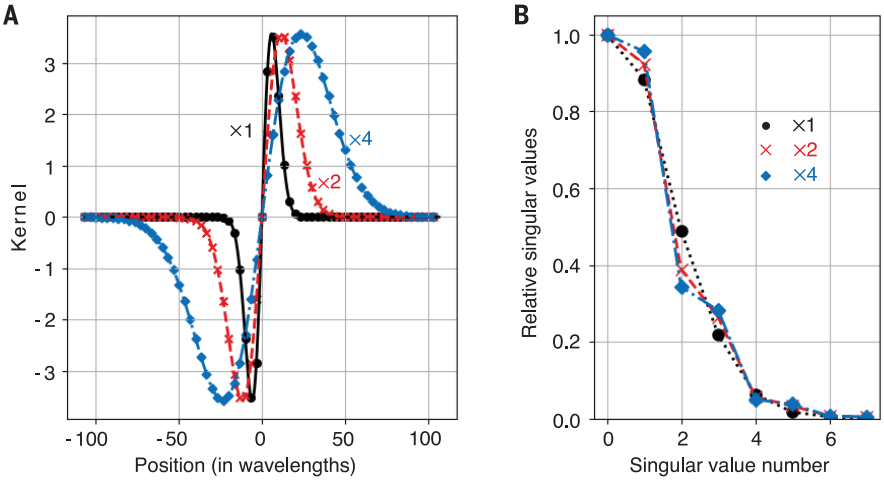

Fig. 3. An "*x* times Gaussian" kernel at three scales. (**A**) The kernels ×1—the original scale—(β = 1) (circles and solid line), ×2 larger (β = 2) (crosses and dashed line), and ×4 larger (β = 4) (diamonds and dot-dashed line). The points correspond to effective sampling points for a numerical aperture NA = 0.15. (**B**) The corresponding relative magnitude of the singular values (including from left-to-right and right-to-left matrices) for the three scales of kernels (with lines as a guide), using symbols and colors as in (A).

Much such metasurface discussion uses k-space (or Fourier) representations of functions and (space-invariant) kernels (*1*, *5*, *6*); pixels are not explicitly used. k-values must be smaller than $k = 2\pi n_r/\lambda_o$ for a propagating wave in the background material with refractive index n_r, or a smaller maximum value $k_{x\max} = 2\pi\mathrm{NA}/\lambda_o$ if the input and output optics has a finite numerical aperture NA. In this case, we can use a sampling theory approach to get effective spatial sampling points (supplementary text S8). With *N* sampling points in one dimension, these are spaced by

$$\delta l = \frac{\lambda_o}{2\mathrm{NA}} \equiv \frac{L}{N} \tag{11}$$

where $L = N\delta l$ now becomes the nominal width of the surfaces for this calculation.

Example calculations of ONL

Pixelated systems

Consider a device implementing a centered finite-difference fifth-order linear derivative (*29*) in the *x* direction, in the spirit of Fig. 1B. Seven adjacent, equally spaced sampling points would have weights proportional to –1, 4, –5, 0, 5, –4, and 1, as sketched in Fig. 2B for a dividing surface between points 7 and 8.

The connections between input points on the right of the dividing surface and output points on the left are expressed by the 3-by-3 matrix

$$\mathbf{D}_{\mathrm{RL}} = \begin{bmatrix} 1 & 0 & 0 \\ -4 & 1 & 0 \\ 5 & -4 & 1 \end{bmatrix} \tag{12}$$

This matrix contains the connections from input points 8, 9, and 10 (corresponding to matrix columns) on the right to output points 5, 6, and 7 (corresponding to matrix rows) on the left. All other connections across the dividing surface are zero. (See supplementary text S9 and fig. S7 for the full matrix $\mathbf{D}$ and matrices $\mathbf{D}_{\mathrm{RL}}$ and $\mathbf{D}_{\mathrm{LR}}$.)

A standard numerical linear algebra calculation of the SVD of $\mathbf{D}_{\mathrm{RL}}$ (using the numpy Python library) gives the three singular values 7.568, 1.684, and 0.080, so $C_{\mathrm{RL}} = 3$. If we similarly analyze the connections from left to right across the dividing surface, from input points 5, 6, and 7 to output points 8, 9, and 10 with this antisymmetric kernel, the resulting matrix ends up being $\mathbf{D}_{\mathrm{LR}} = -\mathbf{D}_{\mathrm{RL}}^{T}$ (fig. S7) and has the same set of three singular values, giving $C_{\mathrm{LR}} = 3$. So, for this fifth-order finite difference derivative, we require $C = C_{\mathrm{RL}} + C_{\mathrm{LR}} = 6$ (as in Eq. 1).

In this SVD, we see an important behavior that we exploit later: Not all the required channels are equally strong, and some may be negligible or nearly so. In fact, the third channel in each direction is nearly 100 times as weak as the first (0.080 compared with 7.568), which suggests that, if we only need a moderately good approximation for our derivative, we might need only two channels in each direction (so $C = 4$).

We can apply the same approach for other pixelated systems; finite impulse response filters and discrete wavelets, such as Daubechies wavelets, give additional examples (supplementary text S10). For pixelated systems, in some simple cases, it is quite straightforward to understand ONL intuitively in optics (supplementary text S11).

Continuous systems

As an example with continuous functions and kernel, we use

$$D(u;x) = \frac{(x-u)}{\beta}\exp\left[-\frac{(x-u)^2}{\beta^2\Delta_t^2}\right] \tag{13}$$

which is a real, 1D version of the "*x* times Gaussian" ∂_x kernel from (*7*) that gives a smoothed differentiation. We allow for a scale-up factor β by which we can increase the distance scale of the kernel, with β = 1 corresponding directly to (*7*). As in (*7*), we take $\Delta_t \simeq 8.325$ wavelengths and NA = 0.15, which, by Eq. 11, leads to sampling points spaced by ~3.33 wavelengths. The resulting kernels for three different scales are shown in Fig. 3 together with the corresponding sets of relative singular values, including both right-to-left and left-to-right singular values in the same graph.

The total number of singular values equals the number of sampling points. After the first several singular values, however, the magnitudes of the remaining ones fall off very rapidly (we plot only the first eight in this work). Also, the set of strongly coupled singular values is essentially the same for all three scales of kernel. Once we have a large number of sampling points over the range where the kernel function is changing substantially, the relative size of the singular values converges. This illustrates that the ONL *C* is a property of the form of the function, not its scale, at least beyond some practical minimum scale. In all three cases shown, only the first six singular values have a relative size >0.01. So, practically, we might choose $C = 6$ for this function.

Thicknesses for space-invariant kernels

These examples show many interesting, discrete, and continuous space-invariant kernels and operations that could be performed with values of *C* from ~4 to ~8. Such numbers are likely still large enough that Eqs. 3 and 4 are usable at least as a first guide. (More sophisticated approaches using SVD are possible for thin structures and/or small *C* without relying on the heuristics behind Eqs. 3 and 4; see supplementary text S12.) Even without DI, such kernels might be implemented practically in structures that, for optical and near-infrared wavelengths, are only some small number of micrometers thick. A comparison with the "*x* times Gaussian" kernel design in (*7*) shows that, with an ~6-wavelength thickness, it also exceeds the minimum required thickness of ~2 wavelengths (supplementary text S13).

Discussion

These examples over a wide range of situations with waves, including pixelated, continuous, space-variant, and space-invariant systems, show that we have a general method to predict

fundamental minimum required thicknesses. The complete process is summarized and some additional discussion is provided in supplementary text S14 and S15, respectively. As illustrated above, systems with optimized designs already approach these limits within some small factor (e.g., a factor of 3 or less).

Flat optical systems offer many interesting possibilities for reducing the thickness of systems—e.g., by using metasurfaces to eliminate most of the thickness of lenses or other elements. This work shows that, especially for applications with large ONL, although we still need thickness overall, much of this thickness just needs to transport optical channels laterally; it may only need to be empty, uniform, or relatively simple waveguiding space, which would simplify overall system design.

REFERENCES AND NOTES

1. C. Guo, H. Wang, S. Fan, *Optica* **7**, 1133–1138 (2020).
2. O. Reshef *et al*., *Nat. Commun.* **12**, 3512 (2021).
3. J. T. R. Pagé, O. Reshef, R. W. Boyd, J. S. Lundeen, *Opt. Express* **30**, 2197–2205 (2022).
4. K. Shastri, O. Reshef, R. W. Boyd, J. S. Lundeen, F. Monticone, *Optica* **9**, 738–745 (2022).
5. A. Chen, F. Monticone, *ACS Photonics* **8**, 1439–1447 (2021).
6. A. Silva *et al*., *Science* **343**, 160–163 (2014).
7. H. Wang *et al*., *ACS Photonics* **9**, 1358–1365 (2022).
8. A. Overvig, A. Alù, *Laser Photonics Rev.* **16**, 2100633 (2022).
9. D. A. B. Miller, *J. Opt. Soc. Am. B* **24**, A1–A18 (2007).
10. D. A. B. Miller, *Phys. Rev. Lett.* **99**, 203903 (2007).
11. M. Gerken, D. A. B. Miller, *Appl. Opt.* **44**, 3349–3357 (2005).
12. Z. Kuang, L. Zhang, O. D. Miller, *Optica* **7**, 1746–1757 (2020).
13. M. I. Abdelrahman, F. Monticone, How Thin and Efficient Can a Metasurface Reflector Be? Universal Bounds on Reflection for Any Direction and Polarization. arXiv:2208.05533 [physics.optics] (2022).
14. P. Chao, B. Strekha, R. Kuate Defo, S. Molesky, A. W. Rodriguez, *Nat. Rev. Phys.* **4**, 543–559 (2022).
15. D. A. B. Miller, *Opt. Express* **20**, 23985–23993 (2012).
16. D. A. B. Miller, *Adv. Opt. Photonics* **11**, 679–825 (2019).
17. N. K. Fontaine *et al*., *Nat. Commun.* **10**, 1865 (2019).
18. S. Pai *et al*., *IEEE J. Sel. Top. Quantum Electron.* **26**, 1–13 (2020).
19. B. J. Shastri *et al*., *Nat. Photonics* **15**, 102–114 (2021).
20. F. Ashtiani, A. J. Geers, F. Aflatouni, *Nature* **606**, 501–506 (2022).
21. X. Lin *et al*., *Science* **361**, 1004–1008 (2018).
22. W. Bogaerts *et al*., *Nature* **586**, 207–216 (2020).
23. G. Wetzstein *et al*., *Nature* **588**, 39–47 (2020).
24. D. A. B. Miller, *Photon. Res.* **1**, 1–15 (2013).
25. D. A. B. Miller, *J. Lightwave Technol.* **35**, 346–396 (2017).
26. V. Blahnik, O. Schindelbeck, *Adv. Opt. Technol.* **10**, 145–232 (2021).
27. J. W. Goodman, *Introduction to Fourier Optics* (Macmillan, 2017).
28. D. A. B. Miller, An introduction to functional analysis for science and engineering. arXiv:1904.02539 [math.FA] (2019).
29. B. Fornberg, *Math. Comput.* **51**, 699–706 (1988).

ACKNOWLEDGMENTS

The author acknowledges stimulating conversations with S. Fan. **Funding:** D.A.B.M. received funding for this work from the MURI program supported by AFOSR grant no. FA9550-21-1-0312. **Competing interests:** The author declares that he has no competing interests. **Data and materials availability:** All data are available in the main text or the supplementary materials.

SUPPLEMENTARY MATERIALS

science.org/doi/10.1126/science.ade3395
Supplementary Text
Figs. S1 to S11
References (*30*–*40*)

Submitted 9 August 2022; accepted 31 October 2022
10.1126/science.ade3395